Chapter 1

Gravity Data Interpretation Using Different New Algorithms: A Comparative Study

Khalid S. Essa and Mahmoud Elhussein

Additional information is available at the end of the chapter

http://dx.doi.org/10.5772/intechopen.71086

Abstract

Gravity data interpretation is useful in exploring regions that have different geological structures, which contain minerals, ores and oil deposits. There are different numerical methods for the model parameters (depth (z), origin location (x_o), shape parameter (q) and amplitude coefficient (A)) evaluation of a covered structure such as gradient method, particle swarm optimization technique and Werner deconvolution method. In this study, application of these methods is utilized to appraise the model parametric quantity of the covered structures. The application of these methods was demonstrated by different engineered data without and with various range of noise (5%, 10%) and applied for a real example from Egypt. The result values of each method were compared together and with those published and drilling information.

Keywords: gravity anomaly, depth, werner deconvolution, PSO, gradient method

1. Introduction

Gravity method is a non-ruinous geophysical procedure that measures contrasts in the gravitational field of the earth at many various areas. It has much beneficial utilization in hydrocarbon exploration, mineral prospecting, archeological investigations, environmental applications and crustal imaging [1–11]. The main objective of the gravity interpretation is evaluating the model parameters (depth, amplitude coefficient, origin location, and shape parameter) of gravity oddities delivered by basic geometrical formed structures (spheres, cylinders). Clarification of gravity data is constantly connected with the ill-posed and non-unique problems. To overcome these issues, we find a preferred geometry to subsurface structures with a known density followed by the inversion processes [12, 13]. Understanding of gravity data can be performed utilizing basic geometrical models, forward modeling and inversion.

Analytical formula for basic geometrical shapes and many approaches have been produced to translate the gravity anomaly expecting the body of basic geometry (sphere, horizontal cylinder and vertical cylinder). These techniques have varying complexity in the interpretation.

All different simple models may not be found in real subsurface geological situations, they usually are preferred in practical inversion of many isolated sources. The target of an inversion process is to recover the converse parameters of the model (depth, amplitude coefficient, origin location and shape factor). Many scientists showed and discussed several graphical and numerical approaches developed in past and significantly in the present time [10, 11, 14–32]. However, the disadvantages of these methods that depend on characteristic points and curves subject to person errors in calculating the inverted parameters of the subsurface structures which can prompt significant errors in assessing the inverse parameters of the covered structure [10, 11]. Thus, the outcomes from these techniques need the accessibility of density information as a noteworthy aspect of the commitment, alongside similar depth information got from geology and/or geophysics. Consequently, the resultant model can shift comprehensively relying upon these factors since the inverse problems are not well-postured and are along these lines unsteady and non-unique [33].

The interpretation of the gravity data is attempted here using three methods: the gradient method [34], the particle swarm optimization and Werner deconvolution method [21]. Analysis of the gravity anomalies can allow obtaining more detailed information on the geological structures that partially outcrops or covered totally in depth. In overall, these different methods are utilized in this work to searching the sources nature of gravity anomalies. The results of applied three different methods are compared together. A synthetic example without and with various level of noise (5% and 10%) used to show the stability of these methods. The proposed techniques are additionally tested on a gravity data from Egypt. To judge satisfaction and fulfillment of these approaches is finished by contrasting the acquired results with other accessible geological or geophysical information in the published literatures.

2. The methods

Different three algorithms used to interpret the gravity anomaly (mGal) produced by most common three shapes (spheres, horizontal cylinders and vertical cylinders) (**Figure 1**) represented by:

$$g(x_i, z, q) = \frac{A}{\left[(x_i - x_o)^2 + z^2\right]^q}, \quad i = 1, 2, 3\ldots\ldots N \tag{1}$$

where

$$A = \begin{cases} \frac{4}{3}\pi G\sigma\, zR^3 \\ 2\pi G\sigma\, zR^2, \\ \pi G\sigma\, R^2 \end{cases} \quad q = \begin{cases} 1.5 & \textit{for a sphere} \\ 1 & \textit{for a horizontal cylinder}. \\ 0.5 & \textit{for a vertical cylinder} \end{cases}$$

http://dx.doi.org/10.5772/intechopen.71086

In the above equation, z is the depth (m), A is the amplitude coefficient (mGal × m^{2q}) that depends on the shape parameter, q is the parameter related to the shape of the body (dimensionless), x_i is the position coordinate (m), x_o is the origin location (m), σ is the density contrast between the target and the surroundings, G is the gravitational constant parameter which equal 6.67×10^{-11} SI units, and R is the radius of the covered body (m), as follow:

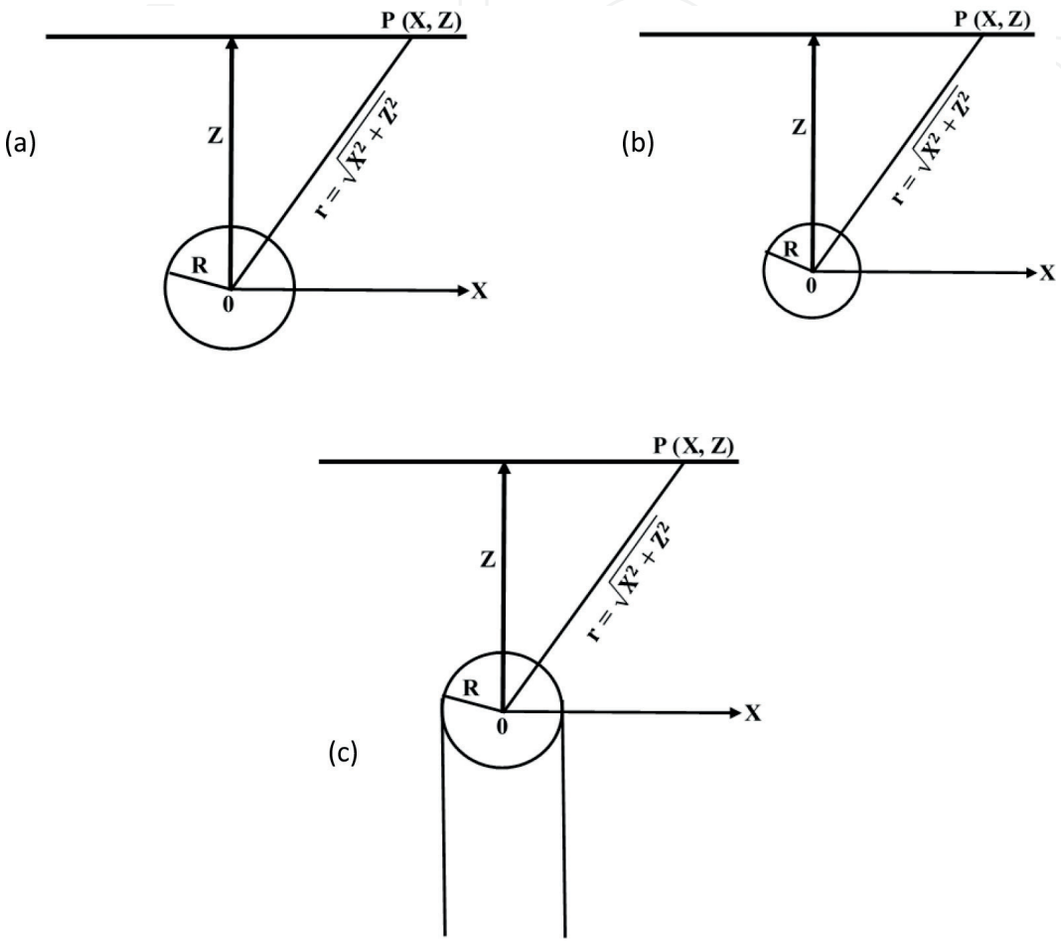

Figure 1. Sketch diagram for different simple geometrical structures: (a) sphere model, (b) horizontal cylinder model and (c) vertical cylinder model.

2.1. The gradient method

The gradient algorithm [34] depends on the utilizing the numerical fourth horizontal gradient registered from the measured gravity anomaly utilizing filter of successive window lengths to evaluate the depth and shape of covered structures. The numerical fourth gradient gravity value at point x_i is figured from measured gravity data $g(x_i)$ by:

$$\Delta g_{xxxx}(x_i) = \frac{\{\Delta g(x_i + 4s) - 4\Delta g(x_i + 2s) + 6\Delta g(x_i) - 4\Delta g(x_i - 2s) + \Delta g(x_i - 4s)\}}{16s^4}, \quad (2)$$

where s is a window length or graticule spacing.

Also, the depth computed using the following form derived from the above equation:

$$F = \frac{A}{16\,s^4}\left(\frac{1}{\left(\left(x_o+4s\right)^2+z^2\right)^q}-\frac{4}{\left(\left(x_o+2s\right)^2+z^2\right)^q}+\frac{6}{\left(x_o{}^2+z^2\right)^q}\right.$$
$$\left.-\frac{4}{\left(\left(x_o-2s\right)^2+z^2\right)^q}+\frac{1}{\left(\left(x_o-4s\right)^2+z^2\right)^q}\right) = 0. \quad (3)$$

2.2. The particle swarm optimization (PSO)

PSO-algorithm was created by [35]. It's relying upon the reenactment of the apparent conducts of birds, fishes and insects in food searching. PSO-algorithm is applied in many issues, like model construction [36], biomedical images [37], electromagnetic optimizations [38] and hydrological problems [39]. In this calculation, the birds representing the particles or models, every molecule has a location vector which speak to the parameters esteem and a velocity vector. So, for a four-dimensional improvement issue, each molecule or individual will have a location in four-dimensional spaces which speak to a solution [40]. Each molecule changes its location at every movement of the operation of the algorithm, this location refreshed amid the iteration procedure considering the best location reached by the molecule which is called the T_{best} model and the best location obtained by any particle in the community called the J_{best} model, this refreshment is clarified in Eqs. (4) and (5) [41]

$$V_i^{k+1} = c_3V_i^k + c_1rand()\left(T_{best}-P_i^{k+1}\right)+c_2rand()\left[\left(J_{best}-P_i^{k+1}\right)P_i^{k+1}\right] = P_i^k+V_i^{k+1}, \quad (4)$$

$$x_i^{k+1} = x_i^k + v_i^{k+1}, \quad (5)$$

where v_i^k is the speed of the molecule *i* at the *k*th cycle, P_i^k is the current I modeling at the *k*th cycle, rand() is an arbitrary number in the vicinity of 0 and 1, c_1 and c_2 are positive constant numbers which ascendency the person and the sociable behavior, they are typically taken as 2 [41] yet some recent researches give that picking c_1 more prominent than c_2 however $c_1 + c_2 \le 4$ may give better outcomes [42], c_3 is the inertial coefficient which control the velocity of the molecule, since the substantial esteems may shuffle the molecules to miss up the great arrangements and the small esteems may bring about insufficient place for exploration [41], it's usually taken less than 1, x_i^k is the positioning of the molecule i at the *k*th cycle.

The four model parameters (z, A, x_o, and q) can be evaluated by using the PSO-algorithm to reach the misfit by using the following objective function:

$$Q = \frac{2\sum_{i=1}^{N}\left|T_i^m-T_i^c\right|}{\sum_{i=1}^{N}\left|T_i^m-T_i^c\right|+\sum_{i=1}^{N}\left|T_i^m+T_i^c\right|}, \quad (6)$$

where N is the number of data points, T_i^m is the observed gravity anomaly, T_i^c is the evaluated gravity anomaly.

2.3. Werner deconvolution method

Werner deconvolution method [21, 43] was also originally developed for magnetic interpretation. Also, Werner deconvolution has been used for gravity interpretation. The method is particularly useful when the profile anomaly of interest can be expressed as a rational function of the form of Eq. (1). As identified by [43], Eq. (1) can be rewritten in linear form as follow:

$$[g(x_i)]^{e_1}(x_i - e_4)^2 + [g(x_i)]^{e_1} e_2 - e_3 = 0, \tag{7}$$

where

$$e_1 = \frac{1}{q},\ e_2 = z^2,\ e_3 = A^{1/q},\ e_4 = x_o.$$

Eq. (7) is linear form in the four variables e_1, e_2, e_3 and e_4, so that a numerically remarkable arrangement can be found for them from evaluating the equation at four points.

The Root Mean Square error (RMS) between the data and model responses is evaluated as follows

$$RMS = \sqrt{\frac{\sum_{i=1}^{N}\left[T_i^m(x_i) - T_i^c(x_i)\right]^2}{N}}. \tag{8}$$

This is considered as a rule in evaluating the best-fitted model parameters (z, A, x_o, q) of the covered structure.

3. Synthetic example

Noisy-free gravity anomaly for a horizontal cylinder with A = 400 mGal m^2, z = 5 m, q = 1, m = 1 and profile length of 120 m. Our analysis begins by applying the fourth horizontal gradient separation technique (Eq. (2)) to the gravity anomaly utilizing distinctive s-values (s = 2, 3, 4 and 5 m) (**Figure 2**). By applying this inversion technique, we evaluated z and A values at different q for every s-value and after that ascertained the average depth and RMS (**Table 1**). **Table 1** exhibits the estimation consequences of the interpretation of noise free data. The assessed parameters from the proposed technique are in a decent concurrence with the model of the horizontal cylinder where z = 5 m, A = 400 mGal m^2 and q = 1. At long last, we can watch that the minimum RMS (RMS = 0 m) occurs at the true model parameters.

Because of the real data are tainted with random noise, random noise of 5 and 10% imposed on the gravity anomaly to see the effect of these noises on the inversion method. The fourth horizontal gradients were evaluated using the same s-values mentioned above (**Figures 3** and **4**). **Table 1** also demonstrates the computational outcomes of the interpretation of noisy gravity data. The average depth of 5 m and the solution with minimum RMS (0.65 mGal) gives in case of 5% noise and depth 4.9 m and RMS of 4.4 mGal in case of 10% noise. This shows that this method is useful when applied to noisy gravity data. In addition, we use

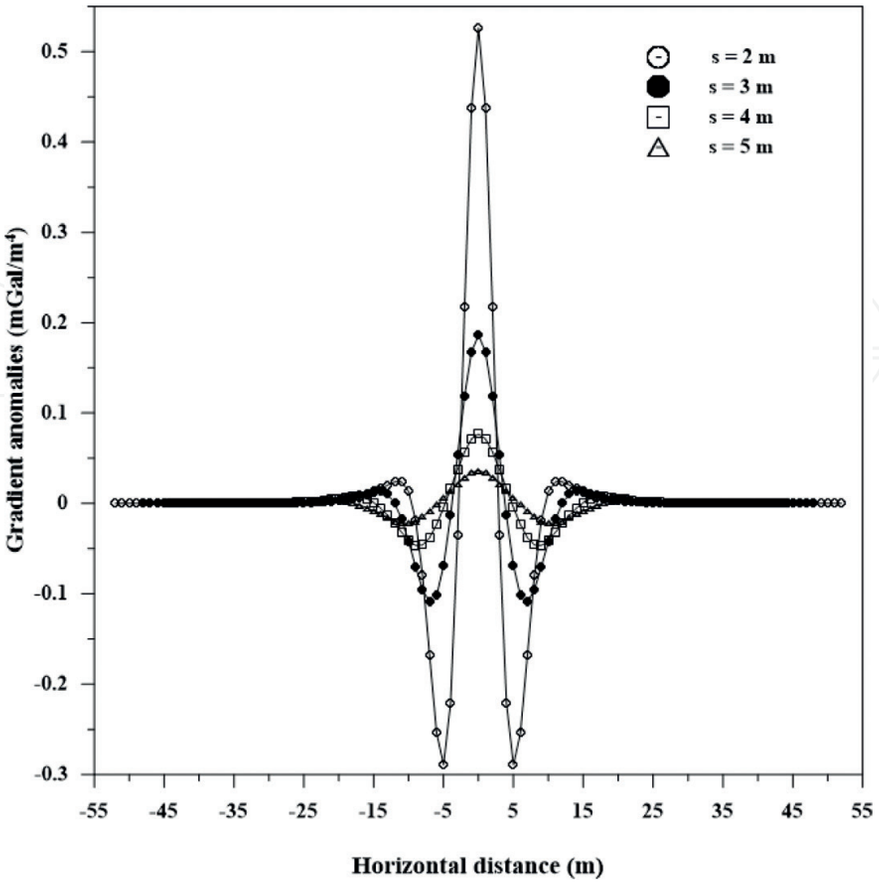

Figure 2. Data analysis of the horizontal cylinder model using the gradient method.

s (m)	Vertical cylinder model, q = 0.5		Horizontal cylinder model, q = 1		Sphere model, q = 1.5	
	z (m)	A (mGal m)	z (m)	A (mGal m^2)	z (m)	A (mGal m^3)
2	3.9	465.8	5	400	4.0	2753.37
3	3.8	461.2	5	400	3.9	3447.5
4	4.1	447.2	5	400	3.9	3916.2
5	4.2	433.1	5	400	4.2	4230.3
Average	4.0	451.9	5	400	4.0	3586.8
RMS (mGal)	17.57		0		25.71	
With 5% random noise						
2	4.2	465.8	5.1	400.0	4.1	2753.3
3	3.7	461.2	4.9	410.5	3.8	3447.5
4	3.8	447.2	5.2	417.7	3.7	3916.2
5	3.9	433.1	4.9	424.6	4.3	4230.2

s (m)	Vertical cylinder model, q = 0.5		Horizontal cylinder model, q = 1		Sphere model, q = 1.5	
	z (m)	A (mGal m)	z (m)	A (mGal m^2)	z (m)	A (mGal m^3)
Average	3.9	451.8	5.0	413.2	3.9	3586.8
RMS (mGal)	17.87		0.65		27.23	
With 10% random noise						
2	4.0	351.7	5.0	479.4	3.9	2079.0
3	4.0	410.5	4.8	481.1	4.0	3068.7
4	4.0	406.3	4.7	432.9	3.9	3557.9
5	3.9	404.2	5.1	422.83	4.0	3947.8
Average	3.9	393.2	4.9	479.4	3.9	3163.4
RMS (mGal)	13.65		4.4		22.29	

Table 1. Numerical results for a gravity model due to horizontal cylinder without and with two levels of 5% and 10% of random noise (A = 400 mGal m^2, z = 5 m, q = 1, and profile length = 120 m) using the gradient method.

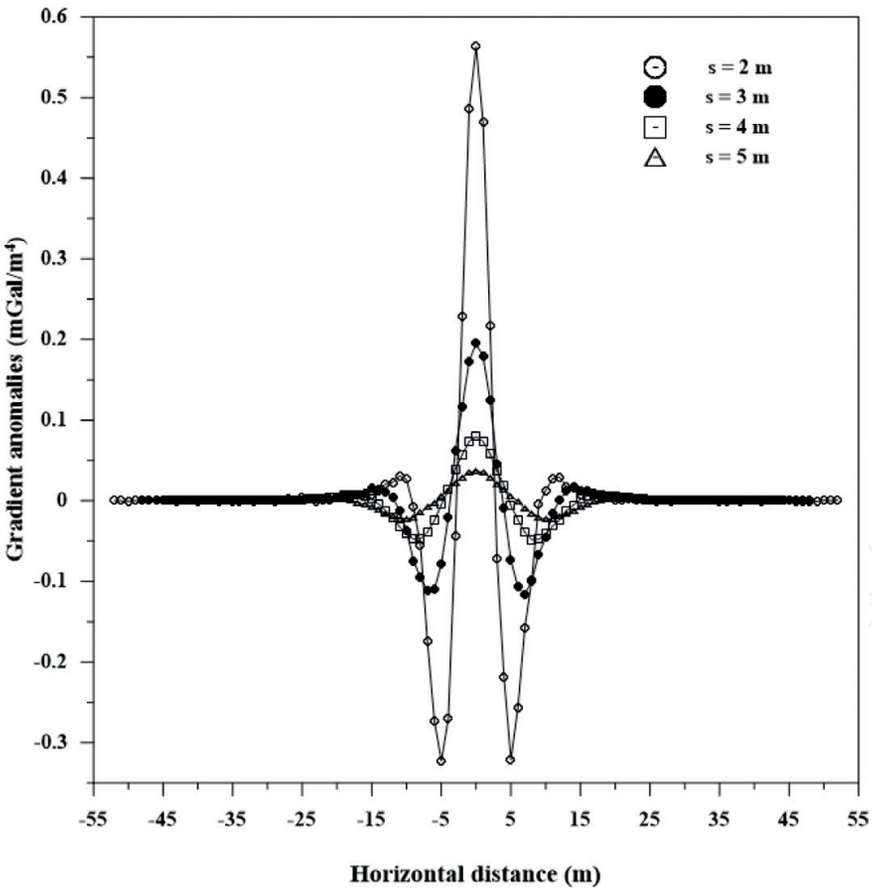

Figure 3. Data analysis of the horizontal cylinder model using the gradient method when the data contain 5% random errors.

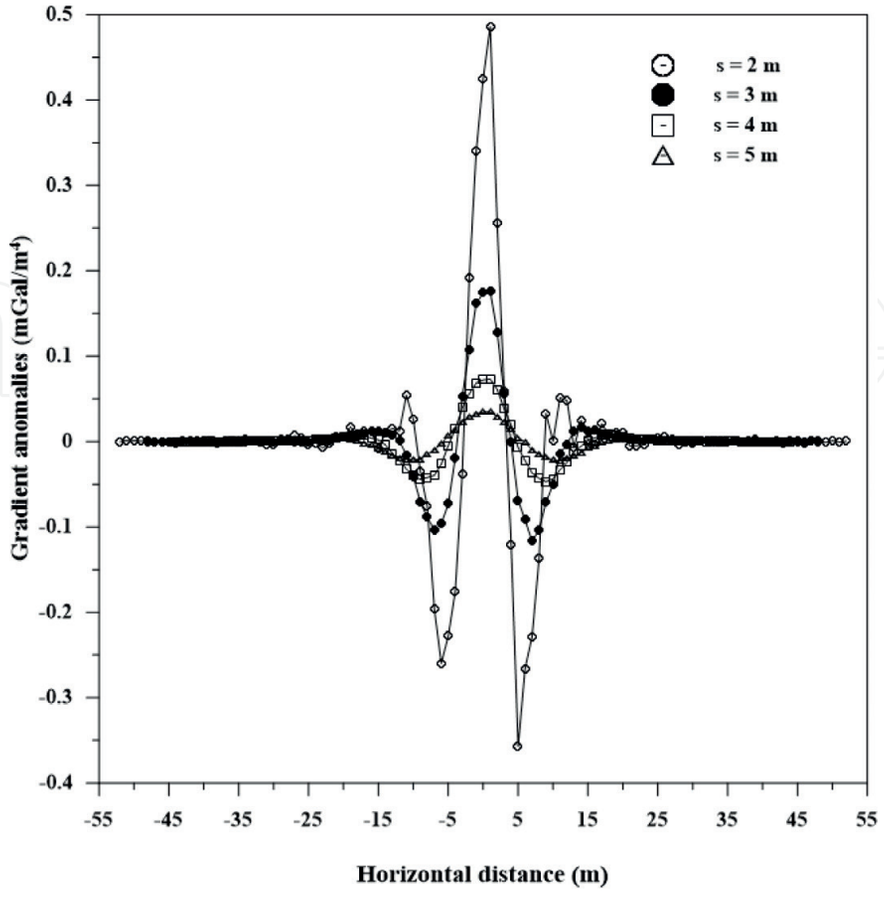

Figure 4. Data analysis of the horizontal cylinder model using the gradient method when the data contain 10% random errors.

Werner deconvolution method to the same gravity anomaly utilizing the same window size every 2 m. we used 11 clustered solutions to calculate the average estimated depth is 5 m, A = 400 mGal m^2, and q = 1 with RMS = 0 mGal. Also, as mentioned above we use the same Werner deconvolution method for the noisy gravity anomalies. The average estimated depth of the cluster solutions is 5.3 m, A = 410.1 mGal m^2 and q = 1 with RMS = 0.82 mGal in case of adding 5% random noise. Also, the average estimated depth of the cluster solutions is 5.6 m, A = 425.3 mGal m^2 and q = 1 with RMS = 1.20 mGal in case of adding 10% random noise (**Table 2**).

The PSO-algorithm was connected to the same synthetic gravity anomaly. In this circumstance, it is noise free data, so we start testing our technique using 100 models. The best model came after 700 cycles, the used extent of the parameters are showed up in **Table 3**. The assessed model parameters which control the body measurements are in good correlation with the proposed values (**Table 3**) corresponding to zero RMS. Since, the uproarious data considered as a basic part in geophysics, thusly, we applied our method to 5% arbitrary random noise gravity data caused by horizontal cylinder model appear with a particular true objective to inquire about the effect of noise corrupted data. The assessed indicate parameters (z, A, x_o, q) are presented in **Table 3**. **Table 3** exhibits that the RMS error is 0.32 mGal. Plus, we forced 10% of subjective random noise on the comparable synthetic anomaly. Also, **Table 3** demonstrates the inverted parameters and shows that the RMS error is 0.64 mGal.

	Vertical cylinder model, q = 0.5			Horizontal cylinder model, q = 1			Sphere model, q = 1.5		
	z (m)	A (mGal m)	x_o (m)	z (m)	A (mGal m²)	x_o (m)	z (m)	A (mGal m³)	x_o (m)
Average	4	458.37	0	5	400	0	3	3875.3	0
RMS (mGal)	18.04			0			55.96		
With 5% random noise									
Average	4.3	465.51	0	5.3	410.1	0	3.4	3884.4	0
RMS (mGal)	17.60			0.82			42.82		
With 10% random noise									
Average	4.5	468.26	0	5.6	425.3	0	3.6	3910.1	0
RMS (mGal)	17.28			1.20			38.25		

Table 2. Numerical results for a gravity model due to horizontal cylinder without and with two levels of 5% and 10% of random noise (A = 400 mGal m², z = 5 m, q = 1, and profile length = 120 m) using Werner deconvolution method.

Type of body	Parameters	Used ranges	Result	RMS (mGal)
	Without random Gaussian noise			
	A (mGal m²)	100–700	400	0
	z (m)	2–12	5	
	q	0–3	1	
	x_o (m)	−20 to 50	0	
	With 5% random Gaussian noise			
	A (mGal m²)	100–700	395	0.32
Horizontal cylinder model	z (m)	2–12	5	
	q	0–3	1	
	x_o (m)	−20 to 50	−0.01	
	With 10% random Gaussian noise			
	A (mGal m²)	100–700	411	0.64
	z (m)	2–12	4.9	
	q	0–3	1	
	x_o (m)	−20 to 50	0.02	

Table 3. Numerical results for a gravity model due to a horizontal cylinder without and with two levels of 5% and 10% of random noise (A = 400 mGal m², z = 5 m, q = 1, x_o = 0 m and profile length = 120 m) using the PSO-technique.

4. Field example

So as to inspect the pertinence and effectiveness of the three showed methods on the real data, we have connected the three techniques to a gravity anomaly profile of Abu Roash dome area,

the Northern Western Desert, Egypt (**Figure 5**). The Bouguer gravity map is situated in the West of Cairo ([44]; his Figure 11) and was mapped in 1980 by the Egyptian General Petroleum Corporation (EGPC) utilizing a density of 2.3 g cm^{-3}. The structure information is accessible from the surface geology and drilled hole data [45]. From the geology information of the area, we observe that the basement rocks (with greater prominent thickness than the above sedimentary layers) are elevated because of the high pressure in the SW direction [45]. At the Abu Roash dome, there are exposures of Cenomanian clastics at its core took after by Turonian and Senonian strata. This Cretaceous succession separated from the above Eocene sediments by an angular unconformity [45–47]. **Figure 5** shows the Bouguer anomaly profile which are opposite to the heading of compression striking NW–SE, this profile was digitized at an interim of 300 m. The Bouguer anomaly accordingly acquired has been subjected to the three various methods (the fourth horizontal gradient method, Werner deconvolution method, and the PSO-technique).

Firstly, we used the fourth horizontal gradient method to four progressive windows (s = 600, 900, 1200 and 1500 m) to obtain the inverted model parameters. The four fourth horizontal gradient anomaly profiles were gotten (**Figure 6**). **Table 4** summarized the results obtained from this method. Secondly, by applying Werner deconvolution method to the same observed gravity data, the outcomes are summarized in **Table 5**. Thirdly, a PSO-algorithm utilized to assess the interpretive model parameters of gravity anomaly profile. **Table 6** displays the ranges and results of the evaluated parameters.

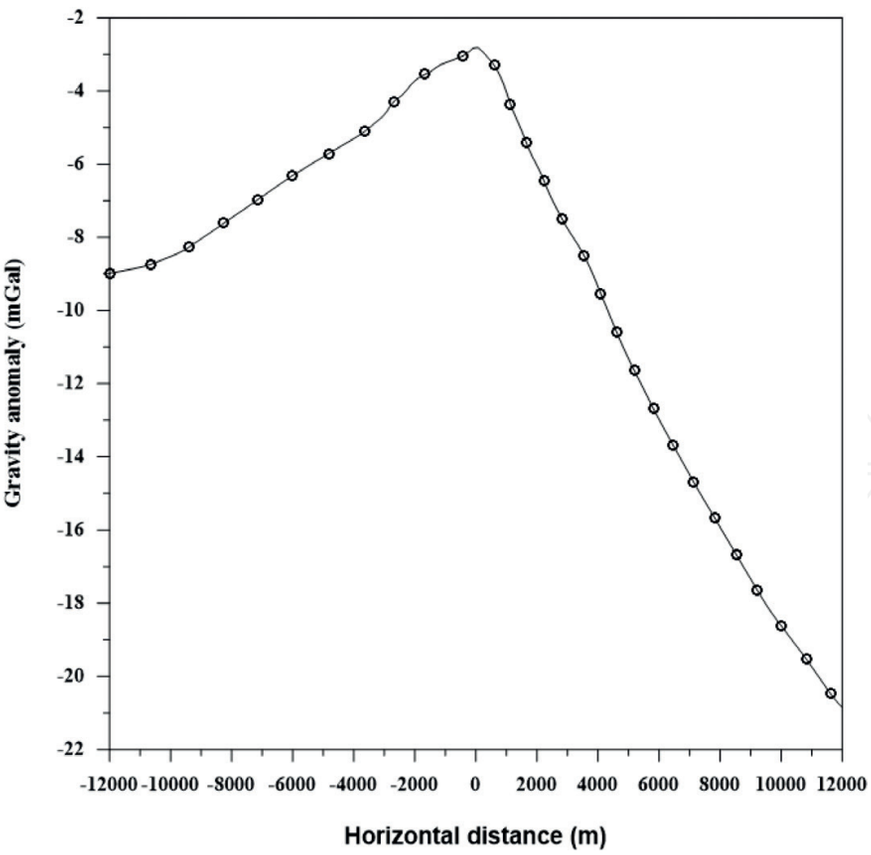

Figure 5. Observed gravity anomaly profile of Abu Roash field example, Egypt.

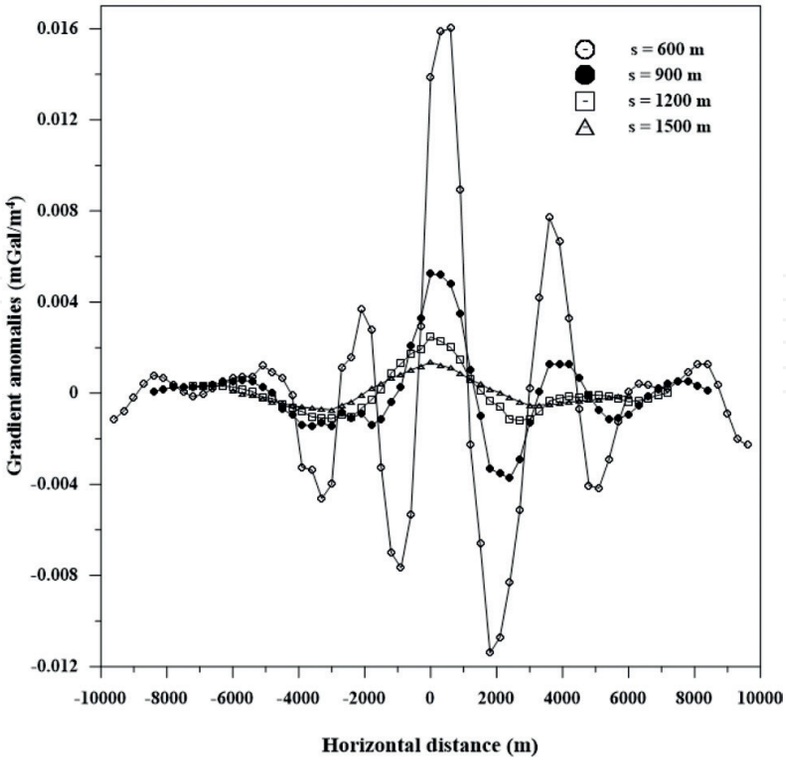

Figure 6. Data analysis of the Abu Roash field example using the present gradient method.

s (m)	Vertical cylinder model, q = 0.5		Horizontal cylinder model, q = 1.0		Sphere model, q = 1.5	
	z (m)	A (mGal m)	z (m)	A (mGal m²)	z (m)	A (mGal m³)
600	1870	−5236	2200	−6160	2520	−13,552,000
900	1890	−5292	2250	−6300	2600	−14,175,000
1200	1920	−5376	2510	−7028	2830	−17,640,280
1500	2050	−5740	2630	−7364	3290	−19,367,320
Average	1932.5	−5411	2397.5	−6713	2810	−16,183,650
RMS (mGal)	10.04		10.38		224	

Table 4. Numerical results of Abu Roash dome field example using the gradient method.

	Vertical cylinder model, q = 0.5			Horizontal cylinder model, q = 1.0			Sphere model, q = 1.5		
	z (m)	A (mGal m)	x_o (m)	z (m)	A (mGal m²)	x_o (m)	z (m)	A (mGal m³)	x_o (m)
Average	1870	−5230	0	2320	−6503	0	2750	−17,253,450	0
RMS (mGal)		10.06			10.39			246.99	

Table 5. Numerical results of Abu Roash dome field example using Werner deconvolution method.

Parameters	Used ranges	Result	RMS (mGal)
A (mGal m)	−2000 to −6000	−5200	0.17
z (m)	500–2500	1860	
q	0–2.5	0.45	
x_o (m)	−100 to 100	0	

Table 6. Numerical results of Abu Roash dome field example using the PSO-technique.

Parameters	Method		Present methods		
	[45]	[48]	Fourth gradient	Werner	PSO
A (mGal m)	1900	1620	−5411	−5230	−5200
z (m)	–	–	1932.5	1870	1860
q (dimensionless)	–	0.5	0.5	0.5	0.45
x_o (m)	–	–	–	0	0

Table 7. Comparison between the present three used method and different methods for Abu Roash field example, Egypt.

Finally, the three inversion techniques give a full picture of the model parameters instead of various techniques which did not give a totally elucidation. The results are outlined in **Table 7**.

5. Conclusions

In this chapter, three various methods were used for modeling gravity anomaly due to simple geometrical shaped. The viability of the proposed methods (the gradient method, particle swarm optimization method and Werner deconvolution method) is used on a synthetic example including noisy-free data, contaminated data with various level of noise (5 and 10%), and a real field data from Egypt. The three approaches can enhance the quality solution and convergence traits and computational adequacy. The examination of the results with drilling information and published information detailed in the literature demonstrated the prevalence of the three methods and its potential for dealing gravity issue. Later on work, we will attempt to suggest some enhanced variant of these methods to deal with issue.

Acknowledgements

We would like to thank Prof. Taher Zouaghi, the Editor, for his keen interest, imperative comments on the Article, and changes to this work. Also, we might want to express gratitude to Ms. Maja Bozicevic, Publishing Process Manager, for her help and collaboration in this issue.

Author details

Khalid S. Essa* and Mahmoud Elhussein

*Address all correspondence to: khalid_sa_essa@yahoo.com

Geophysics Department, Faculty of Science, Cairo University, Giza, Egypt

References

[1] Grant FS, West GF. Interpretation Theory in Applied Geophysics. New York: McGraw-Hill Book Co.; 1965

[2] Roy A. The method of continuation in mining geophysical interpretation. Geoexploration. 1966;**4**:65-83

[3] Nettleton LL. Gravity and Magnetics in Oil Prospecting. New York: McGraw-Hill Book Co.; 1976

[4] Ateya IL, Takemoto S. Gravity inversion modeling across a 2-D dike-like structure—A case study. Earth, Planets and Space. 2002;**54**:791-796

[5] Fedi M. DEXP: A fast method to determine the depth and the structural index of potential fields sources. Geophysics. 2007;**72**(1):I1-I11

[6] Lafehr TR, Nabighian MN. Fundamentals of Gravity Exploration. Tulsa, OK: Society of Exploration Geophysicists; 2012. p. 211

[7] Batista-Rodríguez JA, Pérez-Flores MA, Urrutia-Fucugauchi J. Three-dimensional gravity modeling of Chicxulub Crater structure, constrained with marine seismic data and land boreholes. Earth, Planets and Space. 2013;**65**:973-983

[8] Hinze WJ, Von Frese RRB, Saad AH. Gravity and Magnetic Exploration: Principles, Practices and Applications. New York: Cambridge University Press; 2013

[9] Long LT, Kaufmann RD. Acquisition and Analysis of Terrestrial Gravity Data. New York: Cambridge University Press; 2013

[10] Mehanee SA. Accurate and efficient regularized inversion approach for the interpretation of isolated gravity anomalies. Pure and Applied Geophysics. 2014;**171**:1897-1937

[11] Essa KS. New fast least-squares algorithm for estimating the best-fitting parameters due to simple geometric-structures from gravity anomsalies. Journal of Advanced Research. 2014;**5**(1):57-65

[12] Rama Rao BSR, Murthy IVR. Gravity and Magnetic Methods of Prospecting. New Delhi, India: Arnold-Heinemann Publishers; 1978. p. 390

[13] Chakravarthi V, Sundararajan N. Ridge regression algorithm for gravity inversion of fault structures with variable density. Geophysics. 2004;**69**:1394-1404

[14] Nettleton LL. Gravity and magnetics for geologists and seismologists. AAPG Bulletin. 1962;**46**:1815-1838

[15] Odegard ME, Berg JW. Gravity interpretation using the Fourier integral. Geophysics. 1965;**30**:424-438

[16] Sharma B, Geldart LP. Analysis of gravity anomalies of two-dimensional faults using Fourier transforms. Geophysical Prospecting. 1968;**16**:77-93

[17] Hartman RR, Teskey DJ, Friedberg JL. A system for rapid digital aeromagnetic interpretation. Geophysics. 1971;**36**:891-918

[18] Jain S. An automatic method of direct interpretation of magnetic profiles. Geophysics. 1976;**41**:531-541

[19] Thompson DT. EULDPH—A new technique for making computer-assisted depth estimates from magnetic data. Geophysics. 1982;**47**:31-37

[20] Gupta OP. A least-squares approach to depth determination from gravity data. Geophysics. 1983;**48**:357-360

[21] Kilty KT. Werner deconvolution of profile potential field data. Geophysics. 1983;**48**: 234-237

[22] Lines LR, Treitel S. A review of least-squares inversion and its application to geophysical problems. Geophysical Prospecting. 1984;**32**:159-186

[23] Bowin C, Scheer E, Smith W. Depth estimates from ratios of gravity, geoid, and gravity gradient anomalies. Geophysics. 1986;**51**:123-136

[24] Mohan NL, Anandababu L, Roa S. Gravity interpretation using the Mellin transform. Geophysics. 1986;**51**:114-122

[25] Nandi BK, Shaw RK, Agarwal NP. A short note on identification of the shape of simple causative sources from gravity data. Geophysical Prospecting. 1997;**45**:513-520

[26] Elawadi E, Salem A, Ushijima K. Detection of cavities and tunnels from gravity data using a neural network. Exploration Geophysics. 2004;**32**:204-208

[27] Salem A, Ravat D. A combined analytic signal and Euler method (AN-EUL) for automatic interpretation of magnetic data. Geophysics. 2003;**68**:1952-1961

[28] Essa KS. A simple formula for shape and depth determination from residual gravity anomalies. Acta Geophysica. 2007;**55**:182-190

[29] Asfahani J, Tlas M. An automatic method of direct interpretation of residual gravity anomaly profiles due to spheres and cylinders. Pure and Applied Geophysics. 2008;**165**:981-994

[30] Abedi M, Afshar A, Ardestani VE, Norouzi GH, Lucas C. Application of various methods for 2D inverse modeling of residual gravity anomalies. Acta Geophysica. 2009; **58**:317-336

[31] Asfahani J, Tlas M. Fair function minimization for direct interpretation of residual gravity anomaly profiles due to spheres and cylinders. Pure and Applied Geophysics. 2011;**168**:861-870

[32] Essa KS. A fast interpretation method for inverse modelling of residual gravity anomalies caused by simple geometry. Journal of Geological Research. 2012;**2012** Article ID: 327037

[33] Tarantola A. Inverse Problem Theory and Methods for Model Parameter Estimation. Philadelphia: SIAM; 2005

[34] Essa KS. Gravity data interpretation using the s-curves method. Journal of Geophysics and Engineering. 2007;**4**(2):204-213

[35] Kennedy J, Eberhart R. Particle swarm optimization. In: IEEE International Conference on Neural Networks (Perth, Australia). Vol. IV. Piscataway, NJ: IEEE Service Center; 1998. pp. 1942-1948

[36] Cedeno W, Agrafiotis DK. Using particle swarms for the development of QSAR models based on K-nearest neighbor and kernel regression. Journal of Computer-Aided Molecular Design. 2003;**17**:255-263

[37] Wachowiak MP, Smolíková R, Zheng Y, Zurada JM, Elmaghraby AS. An approach to multimodal biomedical image registration utilizing particle swarm optimization. IEEE Transactions on Evolutionary Computation. 2004;**8**:289-301

[38] Boeringer DW, Werner DH. Particle swarm optimization versus genetic algorithms for phased array synthesis. IEEE Transactions on Antennas and Propagation. 2004;**52**:771-779

[39] Chau WK. Application of a particle swarm optimization algorithm to hydrological problems. In: Robinson LN, editor. Water Resources Research Progress. New York: Nova Science Publishers Inc.; 2008. p. 3-12

[40] Eberhart RC, Shi Y. Particle swarm optimization: Developments, applications and resources. In: Proceedings of the Congress on Evolutionary Computation, Seoul, Korea; 2001. pp. 81-86

[41] Sweilam NH, El-Metwally K, Abdelazeem M. Self potential signal inversion to simple polarized bodies using the particle swarm optimization method: A visibility study. Journal of Applied Geophysics. 2007;**6**:195-208

[42] Parsopoulos KE, Vrahatis MN. Recent approaches to global optimization problems through Particle Swarm Optimization. Natural Computing. 2002;**1**:235-306

[43] Werner S. Interpretation of magnetic anomalies at sheet-like bodies. Sveriges Geologiska Undersok, Series C, Arsbok. 1953;**43**(6)

[44] Abdelrahman EM, Bayoumi AI, Abdelhady YE, Gobashy MM, El-Araby HM. Gravity interpretation using correlation factors between successive least squares residual anomalies. Geophysics. 1989;**54**:1614-1621

[45] Said R. The Geology of Egypt. Amsterdam: Elsevier; 1962

[46] Beadnell HJL. The Cretaceous Region of Abu Roash, near the Pyramids of Giza, Egypt. Cairo: Survey Department; 1902. p. 48

[47] Faris MI. Contributions to the stratigraphy of Abu Roash and the history of the upper Cretaceous in Egypt. Bulletin of Faculty of Science, Cairo University. 1948;**27**:221-239

[48] Abdelrahman EM, El-Araby HM. Shape and depth solutions from gravity data using correlation factors between successive least-squares residuals. Geophysics. 1993;**59**:1785-1791

IntechOpen